A Novel Approach to Nodule Feature Optimization on Thin Section Thoracic CT[1]

Ravi Samala, MS, Wilfrido Moreno, PhD, Yuncheng You, PhD, Wei Qian, PhD

Rationale and Objectives. An analysis for the optimum selection of image features in feature domain to represent lung nodules was performed, with implementation into a classification module of a computer-aided diagnosis system.

Materials and Methods. Forty-two regions of interest obtained from 38 cases with effective diameters of 3 to 8.5 mm were used. On the basis of image characteristics and dimensionality, 11 features were computed. Nonparametric correlation coefficients, multiple regression analysis, and principal-component analysis were used to map the relation between the represented features from four radiologists and the computed features. An artificial neural network was used for the classification of benign and malignant nodules to test the hypothesis obtained from the mapping analysis.

Results. Correlation coefficients ranging from 0.2693 to 0.5178 were obtained between the radiologists' annotations and the computed features. Of the 11 features used, three were found to be redundant when both nodule and non-nodule cases were used, and five were found redundant when nodule or non-nodule cases were used. Combination of analysis from correlation coefficients, regression analysis, principal-component analysis, and the artificial neural network resulted in the selection of optimum features to achieve *F*-test values of 0.821 and 0.643 for malignant and benign nodules, respectively.

Conclusion. This study demonstrates that for the optimum selection of features, each feature should be analyzed individually and collectively to evaluate the impact on the computer-aided diagnosis system on the basis of its class representation. This methodology will ultimately aid in improving the generalization capability of a classification module for early lung cancer diagnosis.

Key Words. Correlation; multiple regression; principal-component analysis; artificial neural network; nodule features.

Computer-aided diagnosis (CAD) for thoracic computed tomographic imaging to detect lung nodules plays a vital role in early cancer diagnosis and thus aids in reducing the mortality rate significantly (1). The most crucial stage in any CAD system is the final classification module, which differentiates malignant lesions from benign lesions using their inherent image characteristics. The input to such a classification module is a set of image features that represent the nodule characteristics. These characteristic features are extracted using a mathematical approach that simulates the human representation of nodule properties.

The Fleischner Society (2) defines a lung nodule from two perspectives. As seen by a pathologist, it is a ''small, approximately spherical, circumscribed focus of abnormal tissue,'' and for a radiologist, it is ''a round opacity, at least moderately well marginated and no greater than 3cm in maximum diameter.'' Non-nodules have a visual presentation that is very similar to nodules but are not cancerous. The assessments of nodule characteristics done by radiologists and pathologists differ from that of the image-processing perspective (3). However, because the image features calculated within a CAD system are motivated largely by a radiologist's perspective, there exists an inherent correlation between human visualization and the mathematical approach to feature characterization.

Mathematically, the features used in a CAD system are well defined for a nodule, but they are not accurate enough

Acad Radiol 2009; 16:418–427

[1] From the College of Engineering (R.S., W.M.) and the College of Arts and Sciences (Y.Y.), University of South Florida, Tampa, FL; and the College of Engineering, University of Texas at El Paso, 500 West University Avenue, El Paso, TX 79968 (W.Q.). Received June 18, 2008; accepted October 15, 2008. **Address correspondence to:** W.Q. e-mail: wqian@utep.edu

doi:10.1016/j.acra.2008.10.009

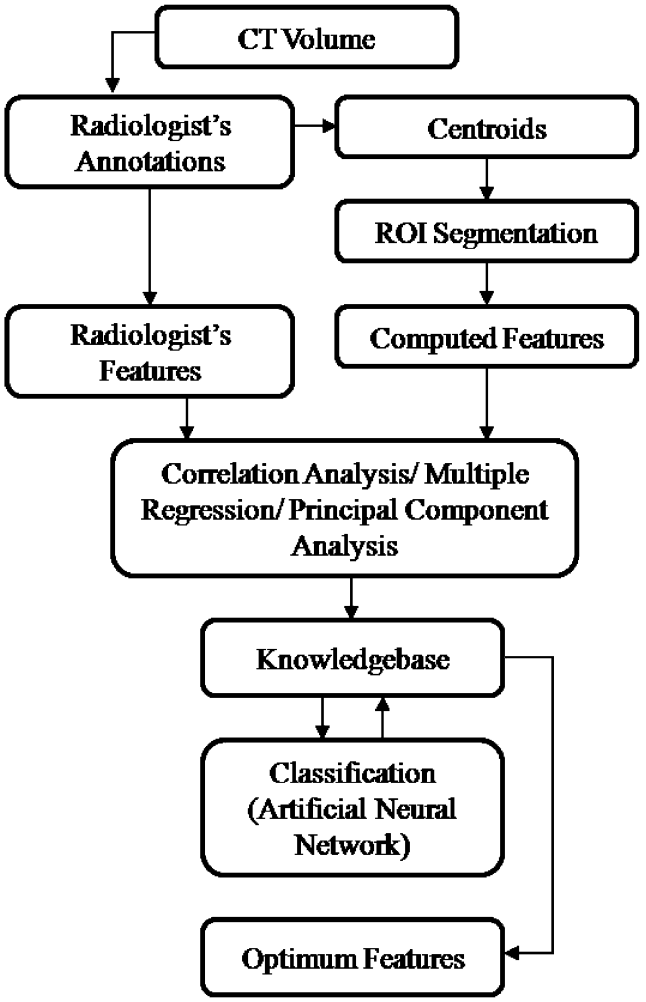

Figure 1. Proposed identification process flowchart. CT, computed tomographic; ROI, region of interest.

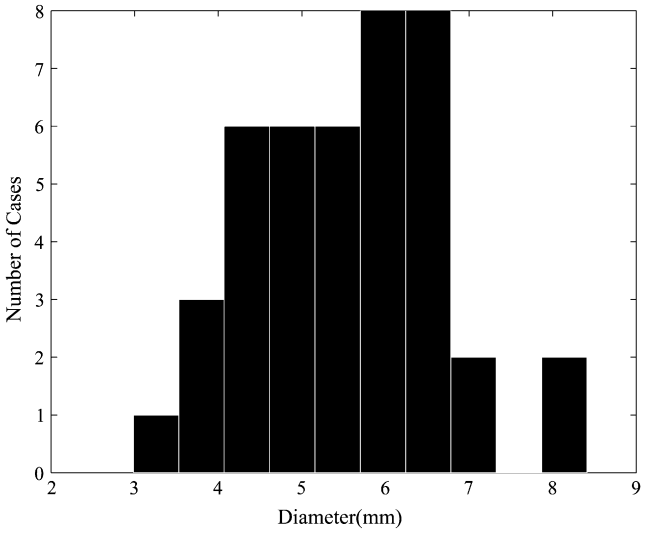

Figure 2. Histogram of nodule size.

to distinguish between a benign and a malignant nodule, which results in a high false-positive detection rate. As pointed out by Sluimer et al (1), currently, much of the research in lung cancer detection is focused on false-positive reduction (ie, to avoid classifying a benign nodule as a malignant nodule). As many as 50 features can be used to detect lung nodules (4–9), but there are disadvantages of using a large number of features to train and test any CAD system, making optimal feature selection an essential process. So far, Aoyama et al (10) have used Wilks's lambda, which is based on in-class variation, to select seven features from a set of 43. Raicu et al (3) used a correlation approach to analyze the mapping between a radiologist's description and computed image features of nodules. However, these methods may not necessarily prove that the mappings can be directly applied to a CAD system. Hence, in addition to correlation analysis, our method exploited the non-nodule characteristics and their inter-relationships and the overall effect on a simple CAD system.

The goal was to find the correlation between image features of a nodule and a non-nodule using the proposed CAD system, as well as the correlation between human- and machine-interpreted features. In this work, we analyze and report the impact of this study on the CAD system's performance. Figure 1 shows the flowchart for this process. Different analyses were performed on the feature relationships, and a rule-based knowledge system was used to select the optimum feature set giving the highest classification accuracy. Briefly, the methodology we present here gives the considerations for selecting optimum features, thus suggesting its general applicability in other CAD-based imaging modalities.

MATERIALS AND METHODS

Database

Thoracic computed tomographic images were obtained from the National Cancer Imaging Archive of the National Cancer Institute (Bethesda, MD). The database is a collection of clinical information initiated by the Lung Imaging Database Consortium (LIDC) to screen patients with lung cancer (11,12). Each patient data set is provided with up to four radiologist annotations (13). The database used for this project consisted of 29 data sets with an in-depth (along the z axis) resolution of <2 mm and nine data sets with an in-depth resolution of 2 to 5 mm. All the images had in-plane resolution (x-y plane) of <1 mm. A total of 42 cases (28 nodules, 14 non-nodules) were used for the feature characterization,

Table 1
Radiologist's Annotations Used by the Lung Imaging Database Consortium

	Feature	Description	Scale
1	Subtlety	Radiologist-assessed subtlety of nodule	1 = extremely subtle, 5 = obvious
2	Internal structure	Radiologist-assessed internal structure score of nodule	1 = soft tissue, 2 = fluid, 3 = fat, 4 = air
3	Calcification	Radiologist-assessed of internal calcification of nodule	1 = popcorn, 2 = laminated, 3 = solid, 4 = noncentral, 5 = central, 6 = absent
4	Sphericity	Radiologist-assessed shape of nodule in terms of its roundness/sphericity, with only three terms defined	1 = linear, 3 = ovoid, 5 = round
5	Margin	Radiologist-assessed margin of nodule, with only the extreme values explicitly defined	1 = poorly defined, 5 = sharp
6	Lobulation	Radiologist-assessed nodule lobulation, with only the extreme values explicitly defined	1 = marked, 5 = no lobulation
7	Spiculation	Radiologist-assessed nodule spiculation, with only the extreme values explicitly defined	1 = marked (marked spiculation), 5 = no spiculation (no spiculation)
8	Texture	Radiologist-assessed nodule internal texture, with only three terms defined	1 = nonsolid/ground class opacity, 3 = part solid/mixed, 5 = solid texture
9	Malignancy	Radiologist subjective assessment of likelihood of malignancy of this nodule (assuming 60-year-old male smoker)	1 = highly unlikely for cancer, 2 = moderately unlikely for cancer, 3 = indeterminate likelihood, 4 = moderately suspicious for cancer, 5 = highly suspicious for cancer

training, and testing phases. The effective diameters of the nodules ranged from 3 to 8.5 mm, as shown in Figure 2.

Nodule Segmentation

The LIDC database provided the region of interest (ROI) of each nodule and the approximate centroid of each non-nodule. Because the non-nodules were not provided with ROIs, we developed a nodule extraction methodology for both nodules and non-nodules, so that the method used to segment ROIs is identical.

The steps in the demarcation of ROIs include calculating the approximate centroid of each nodule, followed by using these centroids as well as the centroids of the non-nodules to segment the three-dimensional region. Adaptive clustering on the basis of directional wavelets (14–16) was adapted to the computed tomographic volume to extract the ROIs around the centroids. The delineation of each nodule always fell somewhere in between the ROIs of the four radiologists, indicating that the accuracy of the segmentation process was within the acceptable standards.

Nodule Characteristics

The definition of a nodule, as defined earlier, is ambiguous, thus leading to the use of multiple feature descriptors. Table 1 lists all the assessment features of the nodule characteristics done by the radiologists in the LIDC collection process.

Table 2
Classification of Image Features Used in the Project

Shape	Size	Intensity	Texture
Sphericity (3D)	Volume (3D)	Mean pixel value (3D)	Contrast (3D)
Maximum compactness (2D)	Area (2D)	SD (3D)	In-plane contrast (2D)
Maximum eccentricity (2D)		Maximum mean pixel value (2D)	
		In-plane SD (2D)	

SD, standard deviation; 3D, three-dimensional; 2D, two-dimensional.

Some of the features are by definition identical between the two perspectives, such as the sphericity and malignancy of radiologists' annotations with the sphericity and volume of the computed features, respectively. For other features, the goal is to find the extent of correlation. The application of this analysis can be used in efficient CAD design, because the optimum selection of nodule features plays an important role in fast and accurate cancer detection. This process will also help reduce the number of input features to the CAD system, to decrease the computational need and decrease classification errors caused by noise. It is also difficult to define accurate decision boundaries in a large dimensional space (''the curse of dimensionality'') (17). As noted by Suzuki et al (18), an increase in the number of features increases the requirement for training cases of an artificial neural network (ANN) classifier

Table 3
Shapiro-Wilk Hypothesis Test for Normality of the Data

Features	*P*	Test ($P < .05$)	Shapiro-Wilk Test Statistic (*W*)
Volume	.6103	0	0.9575
Sphericity	.1006	0	0.9266
Mean	.0000	1	0.6723
SD	.1985	0	0.9381
Contrast	.0000	1	0.6687
Area	.0000	1	0.6471
Compactness	.6468	0	0.9586
Maximum mean	.1422	0	0.9324
Maximum contrast	.0859	0	0.9235
Maximum SD	.0000	1	0.6608
Eccentricity	.0000	1	0.7093

SD, standard deviation.

Table 4
Sphericity Measurements for Figure 5

	Sphericity	
Case	Radiologist	Calculated
1	3	0.1759
2	5	0.1797

exponentially. Thus, the addition of new input features will decrease the accuracy of a classifier. Also, there could be features highly correlated with each other, causing no change in the final accuracy but increasing the computation time.

On the basis of previous experience (13,19), a total of 11 features were used; the careful selection was based on two categories. The first category involved the image characteristics (shape, size, intensity, and texture), and the second category was based on dimensionality (two and three dimensions). These features, as mentioned in Table 2, are the most fundamental of all the features that have been used in the literature so far.

Correlation Analysis

The purpose of this step is to find if each of the radiologists' annotations is mapped to at least one image feature, so that an efficient initial selection of parameters is done. Because it is assumed that the radiologists' annotated features are considered the ''best'' features, high correlation of each computed feature with at least one radiologist's annotated feature improves the confidence level of that particular feature.

Parametric Versus Nonparametric

This step is to decide between the use of parametric and nonparametric correlation coefficients. Among the 11 image features, six followed a normal distribution (parametric), and the remaining five deviated from a normal distribution (nonparametric). Hence, for correlation analysis, instead of the parametric (Pearson's product-moment) correlation coefficient, a nonparametric (Spearman's) correlation coefficient was used. For a database of this size, the Shapiro-Wilk test was chosen to test for non-normality. A significance level of .05 (ie, the deduced hypothesis is true 95% of the time) was used. From Table 3, it is evident that the mean, contrast, area, maximum standard deviation, and eccentricity features deviated from normal distribution (for test = 1). Even though the Shapiro-Wilk test does not guarantee normality, it definitely indicates non-normality.

Table 5
Redundant Features From Principal-Component Analysis

Category	Variation Threshold	Number of Redundant Features
Nodule	2%	5
Non-nodule	2%	5
Both nodule and non-nodule	2%	3
Radiologist	2%	4

Table 6
Classification Results of Three and Two Dimensions and Combined Features

	Correctly Classified	Incorrectly Classified	*F* (nodule)	*F* (non-nodule)
3D	76.1905	23.8095	0.828	0.615
2D	78.5714	21.4286	0.847	0.64
3D and 2D	69.0476	30.9524	0.787	0.435

3D, three-dimensional; 2D, two-dimensional.

Multiple Regression Analysis

This analysis is used to determine the influence of a subset of two- and three-dimensional parameters as a whole on the radiologists' annotations. The general purpose of multiple regression is to learn more about the relationship between several independent (predictor) variables and a dependent (criterion) variable. In this case, it is used to understand which computed image feature has the greatest effect on a particular radiologist's annotation when modeled with all the image features.

Classification

For any classification problem, a given image feature is considered to be good only if it has enough information to distinguish between classes. A single feature by itself is insufficient for classification; several features are used

Table 7
Classification Using All Features Except Maximum Eccentricity

	Correctly Classified	Incorrectly Classified	*F* (nodule)	*F* (non-nodule)	Correlation with Radiologist
All but maximum eccentricity	69.0476	30.9524	0.787	0.435	0.2693

Table 8
***F*-Test Results for Various Features**

Features	*F* (nodule)	*F* (non-nodule)	Correlation with Radiologist
All computed features	0.8	0.5	N/A
Volume	0.8	0	0.5027
Contrast	0.8	0	0.3739
Compactness	0.765	0	0.5178
Sphericity	0.75	0.5	0.4586
Area	0.831	0.421	0.4739
Maximum contrast	0.767	0.417	0.3397
Maximum eccentricity	0.733	0.333	0.2693
Mean	0.698	0.095	0.4947
SD	0.698	0.095	0.4123
Maximum mean	0.698	0.095	0.4675
Maximum SD	0.738	0.105	0.3961
Sphericity, area, maximum contrast, maximum eccentricity	0.821	0.643	N/A
Volume, compactness, contrast	0.781	0.3	N/A

N/A, not available; SD, standard deviation.

Table 9
***F*-Test Results Using All Features Except Those Mentioned in the Table**

All Features Excluding	*F* (nodule)	*F* (non-nodule)
Volume	0.8	0.5
Sphericity	0.814	0.56
Mean	0.822	0.522
SD	0.759	0.462
Contrast	0.793	0.538
Area	0.833	0.583
Compactness	0.8	0.5
Maximum mean	0.8	0.5
Maximum contrast	0.833	0.583
Maximum eccentricity	0.787	0.435
Maximum SD	0.759	0.462

SD, standard deviation.

by various classification algorithms. Ideally, the correlation analysis between the image features and the annotations is considered to improve CAD performance. This analysis was used in the selection of features that best define the distinction between a nodule and a non-nodule.

However, for a classification algorithm used in a CAD system, the representation of a nodule as well as a non-nodule needs to be used for training. Finding the correlation between annotated and calculated descriptors of a nodule alone is insufficient to classify benign and malignant nodules.

To test the hypothesis from correlation analysis, a three-layer feed-forward neural network with a nonlinear sigmoid activation function using a back-propagation learning algorithm was used to classify the abnormal and normal lung nodules. The objective of the classification step was to verify which combination of features resulted in the best class representation but not to improve the overall CAD performance at this point. This helps in rating the input image features toward efficient classification. A *k*-fold cross validation with 500 iterations was used for all the combinations of input features. In this method, the data set is divided into k parts, with $k - 1$ parts used for training and the remaining part used as a testing set. This process is repeated k times, with the constraint that each part is used exactly once for testing. This ensures that all the data are effectively used for both training and testing purposes in case of a small data set. A k value of 4 was chosen to divide the training and testing sets into 75% and 25%, respectively. The parameter F test was used for this purpose to grade the quality of each class representation after testing process. The closer the value of F is to 1, the better is the representation of the class.

Knowledge Base

Knowledge base is an intermediate process to decide whether the results from correlation analysis can be used to select the optimum features. All the results of correlation analysis, multiple regression, and principal-component analysis (PCA) are tested to determine the effectiveness toward classification. Hence, as a first step, all the features are individually used to train and test the classification algorithm. This will result in effectiveness of each feature toward individual output class representation. Next, all the features with the highest correlation coefficients are used as input features. This is the case where it is accepted that all the highly correlated features will in fact result in good classification. All

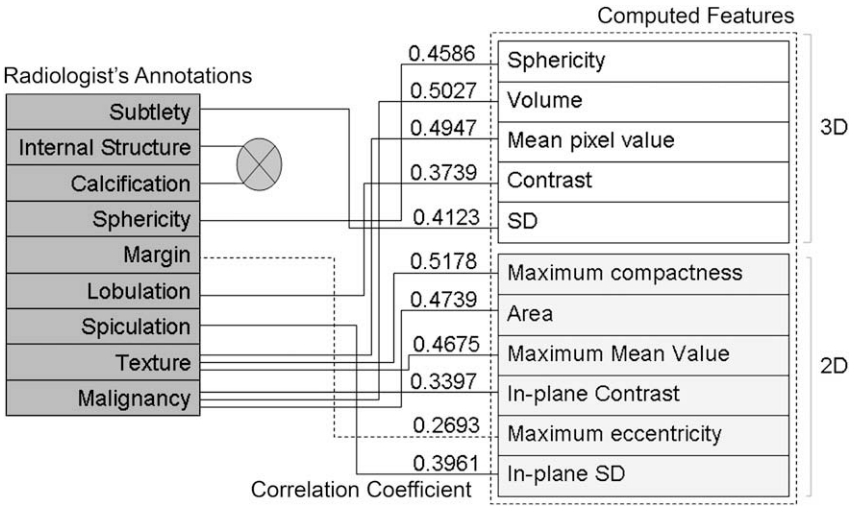

Figure 3. Correlation analysis between computed features and radiologists' annotations. Parametric correlation coefficient values are used to show the strength of mapping. SD, standard deviation; 3D, three-dimensional; 2D, two-dimensional.

features except for one feature as an input are used, repeating this for the number of features, eliminating one feature each time. It is a way to analyze the impact of one feature when all the features are used. Then, combinations of three- and two-dimensional features are used, storing the F values every time. This is to analyze how multiple regression analysis can affect the selection of features.

One combination of features that the knowledge base selects is based on the feedback from the ANN. The selection of these features is based on the F values when an individual feature is used for training and testing the ANN. The feature that represents the nodule and the non-nodule class by >50% of the maximum attained F value for any feature is selected. Then, the results of PCA are used to cross-check for any redundant features in the selected subset. If two features are found redundant, then the feature with highest average of F values for both classes is used instead.

RESULTS

The interobserver variation among radiologist assessments when characterizing a nodule is apparent (20–22). This results in data that are partially random and without conformity, thus producing low values of correlation coefficients, as seen in Figure 3. These findings correlate with previous results (2,11). The variation is evident in the data we selected; one such example is shown in Figure 4, in which all four radiologists marked the ROIs differently. Sphericity and volume calculated from the ROIs in Figure 4 and the sphericity as indicated by the radiologists in Figure 5 show the severity of the extent of variation. In Figure 6 and Table 4, the calculated sphericity is compared with the annotated sphericity for two different nodules. Although the calculated sphericities were equal, the annotated sphericities differed by two levels. Figure 7 shows the variation between observed and calculated sphericities over the entire data set. For each level of observed sphericity, the calculated sphericity varied from a minimum to a maximum value. This suggests that the direct use of the radiologist annotations for a classification algorithm is likely to result in an erroneous diagnosis.

PCA was used to find the presence of any redundant features (Table 5) among the nodule and non-nodules. A variation threshold of 2% was used to estimate the number of redundant features.

Multiple regression analysis of subsets of five three-dimensional, five two-dimensional, 10 three-dimensional and two-dimensional, and 11 features can be visualized using squared multiple correlation coefficients (R^2). If $R^2 = 0$, a model has no predictability, and if $R^2 = 1$, a model has perfect predictability. Looking at the graph (Fig 8), it can be concluded that the higher the number of features, the better the predictability of the model. Although this is the case, it is possible that with more features, the classification algorithm may not be generalized enough, and the accuracy of correct classification could be lower.

The feedback from the ANN classification algorithm in conjunction with the knowledge base leads to the results presented in Tables 6 to 9. Table 6 gives the impact of two- and three-dimensional features on the classification module. The effect of the maximum eccentricity feature that had the lowest correlation coefficient is shown in Table 7, and the

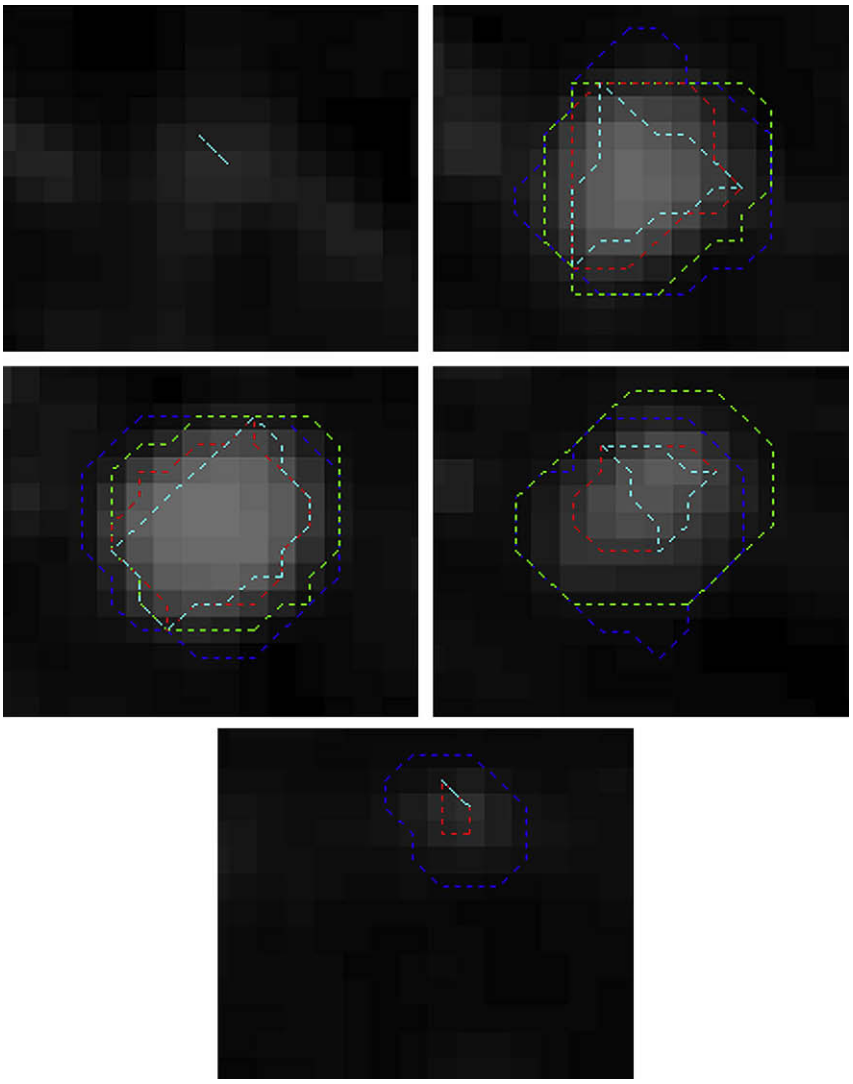

Figure 4. Regions of interest as marked by four different radiologists *(blue, green, red, and cyan lines)* for a nodule on consecutive slices shown along the in-depth *(z)* direction.

effect of each feature is shown in Table 8. Table 9 gives the F values of the all features used collectively, excluding the feature mentioned in the table.

DISCUSSION

The level of impact of human visualization on the development of CAD systems is an area that needs to be explored. This will help determine to what extent current CAD methods are dependent on the human approach of analyzing radiographic images. By using more image features, the probability of identifying a nodule is higher. However, given the nature of a classification methodology, the use of a large number of features will increase the false-positive rate and computation time and would probably result in overtraining.

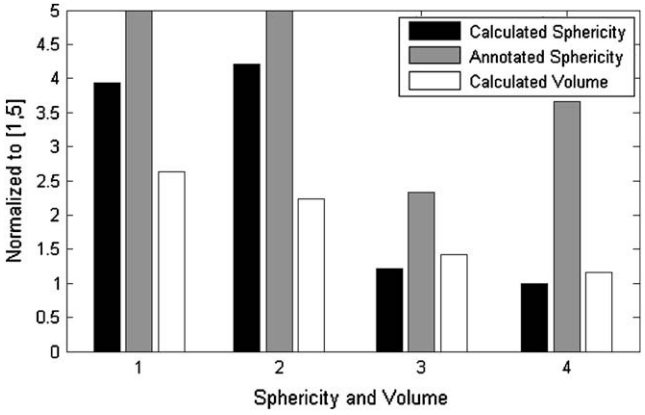

Figure 5. Sphericity measured by different radiologists and calculated along with the volume of the nodule.

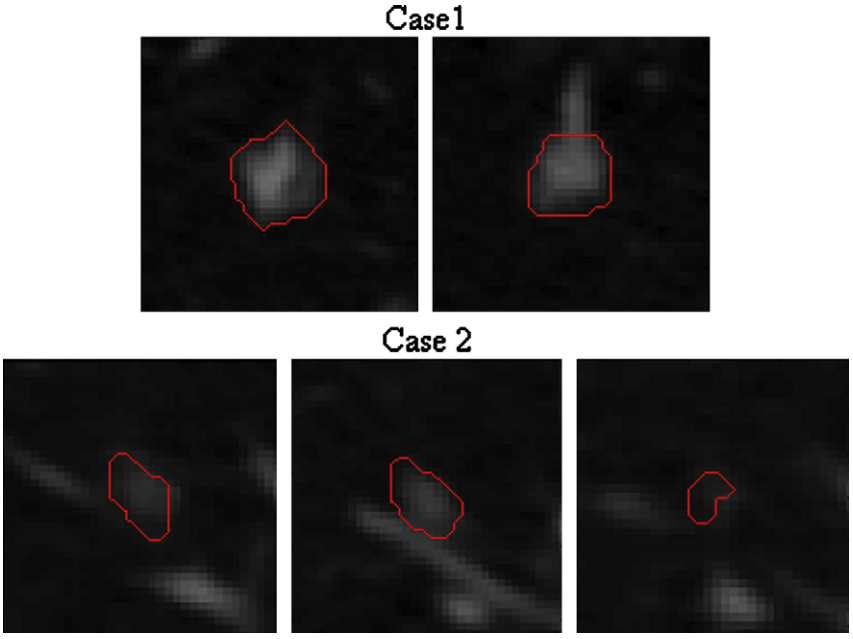

Figure 6. Two different nodule cases with equal calculated sphericities but unequal annotated sphericity values as indicated in Table 6. Consecutive slices along the in-depth (*z*) direction are shown.

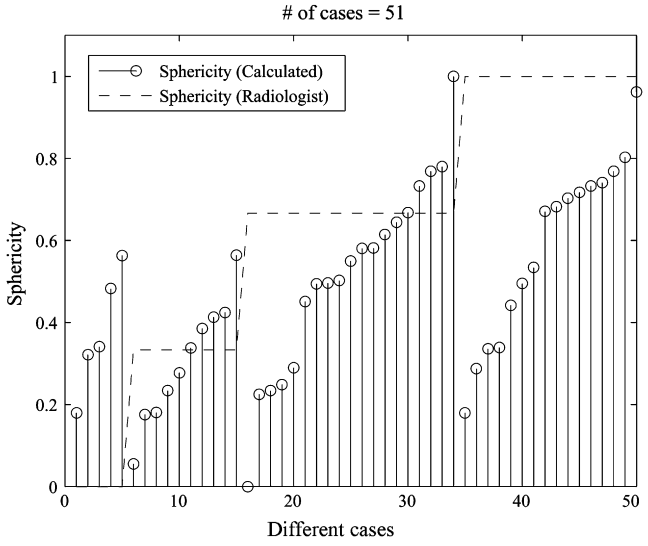

Figure 7. Radiologist's assessment of sphericity versus machine-calculated sphericity.

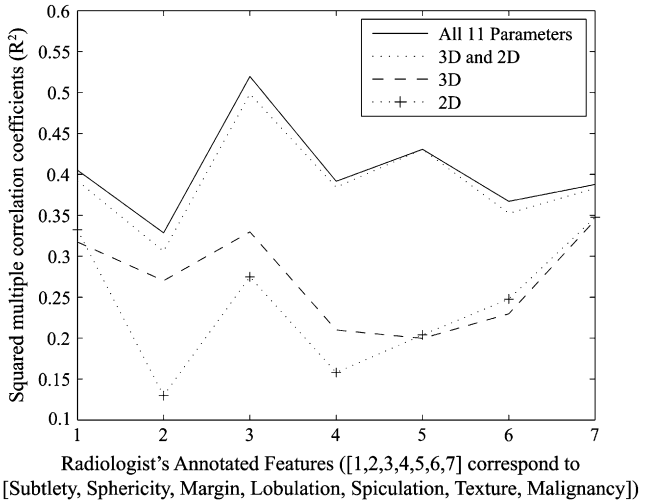

Figure 8. Multiple regression analysis results for two-dimensional (2D) and three-dimensional (3D) parameters. The *x* axis is the radiologist's annotations, and the *y* axis represents the square of the correlation coefficient (R^2).

Three different analyses—correlation, multiple regression, and PCA—were performed to observe the type and strength of the mapping between the annotations and the calculated image features. Each analysis resulted in framing the rules and constraints for the selection of the best image features that were optimum descriptors for a classification method. These rules were tested with ANN classification, whose feedback was used to obtain the best optimum features from the CAD system's perspective. The effect of the strength of mappings on the CAD system was analyzed in detail.

Correlation analysis can be used to see if the computed features have any correlation with the radiologists' annotations. This will help determine if the selected machine

features are as good as the human visual descriptors in identifying the cancerous tissue. At this step, care must be taken to be certain that at least one computed feature is highly correlated with each of the radiologists' annotations. This step will generally help increase the in-class representation of the nodule.

From multiple regression analysis, it can be concluded that the subset of two-dimensional features influenced the final prediction model better than that of the three-dimensional features. In addition, any increase in the number of parameters resulted in an increase in the correlation coefficient for each linear prediction model. Hence, it is recommended to use more two-dimensional computed features than three-dimensional features for nonisometric volume. From PCA, up to three redundant features were observed, indicating the presence of highly correlated features. Reducing the redundant features principally improves the computation time for the training and testing phases of the classification module.

A classification algorithm is used to test the weights of the hypotheses from correlation, multiple regression, and PCA. From Figure 3, maximum eccentricity was observed to have a high impact on the F test for a non-nodule class (Tables 7 and 9) when the feature was eliminated from the classification, even though it had the lowest correlation coefficient. Hence, it can be concluded that maximum eccentricity is one image feature that is a good representation of a non-nodule among all the features that were used. Features such as volume, compactness, and mean had the highest correlation coefficients, but when used individually for classification (Table 8), the F value for in-class representation of non-nodules was found to be zero. Similarly, when these features were removed from the classification stage, the F values were unaffected (Table 9). Thus, correlation analysis cannot be used entirely as a precursor for feature selection.

As shown in Table 6, two-dimensional features are better descriptors to distinguish a nodule and a non-nodule compared with three-dimensional features. The F values for each class are high in case of the two-dimensional features. This could be attributed to the nonisometric resolution of the data. It was also observed that combining the two- and three-dimensional features resulted in lower F values for each class, indicating the presence of noise. From Table 9, it was observed that by removing each feature from the pool of all the features, the in-class representation sometimes improved or worsened or did not change at all, indicating that multiple regression analysis cannot be entirely relied on to select the optimum features.

The knowledge base module is programmed to select features with high F values for both classes, to include more two-dimensional features compared with three-dimensional features, and to eliminate any features with high correlation among themselves. The highest F values were achieved when sphericity, area, maximum contrast, and maximum eccentricity features were used (Table 8). These features had neither the highest nor the lowest correlation coefficients; rather, 75% belonged to the two-dimensional category and 25% belonged to the three-dimensional category. To test this premise, volume, compactness, and contrast features that did not represent the non-nodule class were used, resulting in low F values.

Beside the ANN classifier and the three analyses used for the selection of features in thoracic computed tomographic data, we shall explore some other analyses on the basis of mathematical programming. Classification of biopsy lung tissue images (23) will be tested for the general application of this methodology. An extension of robust linear programming (24,25) can be used for this kind of optimal feature selection.

In conclusion, CAD developers should not include features depending on various analyses oriented toward radiologist annotations alone. Each feature must be analyzed to evaluate the impact it has on the CAD system on the basis of its class representation. The generalization capability of a classification methodology will be limited if the selection of features is based solely on radiologists' nature of analyzing lung nodules. Features from different dimensionality and domains should be considered as an initial feature set, to describe vaguely defined nodules. The mappings between radiologists and CAD developers will create a common platform that can be used to enhance meaningful communication. This will motivate radiologists to assess pulmonary nodules from a different perspective. The present analyses are generalized to be used in any CAD system, provided that training and testing are involved in the classification process.

REFERENCES

1. Sluimer I, Schilham A, Prokop M, et al. Computer analysis of computed tomography scans of the lung: a survey. IEEE Trans Med Imaging 2006; 25:385–405.
2. Austin JH, Müller N, Friedman PJ, et al. Glossary of terms for CT of the lungs: recommendations of the nomenclature committee of the Fleischner Society. Radiology 1996; 200:327–331.
3. Raicu DS, Varutbangkul E, Cisneros JG, et al. Semantics and image content integration for pulmonary nodule interpretation in thoracic computed tomography. Proc SPIE Int Soc Opt Eng 2007; 8: 65120S.1–65120S.12.
4. Armato SG III, Li F, Giger ML, et al. Lung cancer: performance of automated lung nodule detection applied to cancers missed in a CT screening program. Radiology 2002; 225:685–692.
5. Brown MS, Goldin JG, Suh RD, et al. Lung micronodules: automated method for detection at thin-section CT—initial experience. Radiology 2003; 226:256–262.
6. Lee Y, Hara T, Fujita H, et al. Automated detection of pulmonary nodules in helical CT images based on an improved template-matching technique. IEEE Trans Med Imaging 2001; 20:595–604.
7. Tong J, Da-Zhe Z, Jin-Zhu Y, et al. Automated detection of pulmonary nodules in HRCT images. In: Proceedings of the 1st International

Conference on Bioinformatics and Biomedical Engineering. New York: IEEE, 2007:833–836.
8. Armato SG III, Giger ML, Moran CJ, et al. Computerized detection of pulmonary nodules on CT scans. RadioGraphics 1999; 19:1303–1311.
9. McNitt-Gray MF, Wyckoff N, Sayre JW, et al. The effects of co-occurrence matrix based texture parameters on the classification of solitary pulmonary nodules imaged on computed tomography. Comput Med Imag Graphics 1999; 23:339–348.
10. Aoyama M, Li Q, Katsuragawa S, et al. Computerized scheme for determination of the likelihood measure of malignancy for pulmonary nodules on low-dose CT images. Med Phys 2003; 30:387–394.
11. Clarke LP, Croft BY, Staab E, et al. National Cancer Institute initiative: lung image database resource for imaging research. Acad Radiol 2001; 8:447–450.
12. Armato SG III, McLennan G, McNitt-Gray MF. Lung Image Database Consortium: developing a resource for the medical imaging research community. Radiology 2004; 232:739–748.
13. McNitt-Gray MF, Armato SG III, Meyer CR. The Lung Image Database Consortium (LIDC) data collection process for nodule detection and annotation. Acad Radiol 2007; 14:1464–1474.
14. Qian W, Li LH, Clarke LP. Image feature extraction for mass detection using digital mammography: influence of wavelet analysis. Med Phys 1999; 26:402–408.
15. Qian W, Sun XJ, Song DS, et al. Digital mammography: wavelet transform and Kalman filtering neural network in mass segmentation and detection. Acad Radiol 2001; 11:1074–1082.
16. Qian W, Lei M, Song DS, et al. Computer aided mass detection based on ipsilateral multi-view mammograms. Acad Radiol 2007; 14: 530–538.
17. Fukunaga K. Introduction to statistical pattern recognition. London: Academic Press, 1990.
18. Suzuki K, Feng Li, Sone S, et al. Computer-aided diagnostic scheme for distinction between benign and malignant nodules in thoracic low-dose CT by use of massive training artificial neural network. IEEE Trans Med Imaging 2005; 24:1138–1150.
19. Qian W, Zhukov TA, Song DS, et al. Computerized analysis of cellular features and biomarkers for cytologic diagnosis of early lung cancer. Anal Quant Cytol Histol 2007; 10:18–28.
20. Dodd LE, Wagner RF. Armato SG III. Assessment methodologies and statistical issues for computer-aided diagnosis of lung nodules in computed tomography: contemporary research topics relevant to the Lung Image Database Consortium. Acad Radiol 2004; 11: 462–475.
21. Meyer CR, Johnson TD, McLennan G. Evaluation of lung MDCT nodule annotation across radiologists and methods. Acad Radiol 2006; 13: 1254–1265.
22. Armato SG III, McNitt-Gray MF, Reeves AP. The Lung Image Database Consortium (LIDC): an evaluation of radiologist variability in the identification of lung nodules on CT scans. Acad Radiol 2007; 14: 1409–1421.
23. Land WL, McKee DW, Zhukov T, Qian W. A kernelised fuzzy-support vector machine CAD system for the diagnosis of lung cancer from tissue images. Int J Funct Informat Pers Med 2008; 1:26–42.
24. Bennett KP, Mangasarian OL. Robust linear programming discrimination of two linearly inseparable sets. Optim Methods Softw 1992; 1: 23–34.
25. Mangasarian OL. Mathematical programming in data mining. Data Min Knowl Discov 1997; 42:183–201.

Erratum

''Asymmetry Analysis in Rodent Cerebral Ischemia Models.'' Acad Radiol 2008; 15:1181–1197.

In the section ''Materials and Methods'' (pp 1183–1187), the included mathematics closely parallels the development in the unpublished manuscript ''Further Techniques for Enhancing Asymmetry in Brain Imagery,'' by X. Liu, C. Imielinska, and J. Rosiene (2005), without reference to the prior work. The authors regret the omission.